Rotational structure and magnetic g factors of $O_2(X^3\Sigma_g^-, v = 0)$ from laser-magnetic-resonance spectra

Liviu Tomuta and Masataka Mizushima
Department of Physics and Astrophysics, University of Colorado, Boulder, Colorado 80302

Carleton J. Howard
Aeronomy Laboratory, NOAA, Environmental Research Laboratory, Boulder, Colorado 80302

K. M. Evenson
Time and Frequency Division, National Bureau of Standards, Boulder, Colorado 80302

(Received 20 March 1975)

Using the 108- and 84-μm D_2O laser lines, new laser-magnetic-resonance (LMR) spectra of the oxygen molecule in its ground state ($X^3\Sigma_g^-, v = 0$) are observed and analyzed. The corresponding transitions are $n = 15 \rightarrow 17$ and $n = 19 \rightarrow 21$, respectively. Bauer, Kamper, and Lustig's values of the g factors are consistent with our results, but Hendrie and Kusch's values are not. Combining all LMR results with other results, we obtain rotational parameters $B_0 = 43.1004608(75)$ GHz and $B_1 = -0.145\,20(20)$ MHz.

In this paper we report new laser-magnetic-resonance (LMR) measurements and resulting rotational constants of the oxygen molecule in its ground state ($X^3\Sigma_g^-, v = 0$), obtained by using the 108- and 84-μm D_2O laser lines.

The first gas-phase LMR spectrum was observed by Evenson, Broida, Wells, Mahler, and Mizushima[1] on the $n = 3 \rightarrow 5$ transition of the oxygen molecule using the 337-μm HCN laser line. The same LMR spectrum was later measured more accurately by Mizushima, Wells, Evenson, and Welch.[2] Evenson and Mizushima[3] observed LMR spectra of this molecule using the 119- and 78-μm H_2O laser lines, which correspond to the $n = 13 \rightarrow 15$ and $n = 21 \rightarrow 23$ transitions. The present experimental arrangements are the same as reported earlier,[2,3] except that a D_2O laser is used as the radiation source, instead of the previous HCN and H_2O lasers. Figure 1 shows the rotational transitions observed by means of LMR, along with the $n = 1 \rightarrow 3$ transition observed in submillimeter spectroscopy by McKnight and Gordy,[4] and Steinbach and Gordy.[5] In addition, many of the fine-structure splittings of rotational levels in O_2 have been observed in microwave spectroscopy.[6]

The LMR recorder traces for the 108-μm D_2O laser line (2783.0666 GHz) are shown in Fig. 2, where $\mathcal{B}$ and $\mathcal{B}_\omega$ are the external magnetic field and the magnetic component of the laser radiation field, respectively. There are two series of resonance lines; the low-field series is the transition $(n = J = 15) \rightarrow (n = 17, J = 16)$, while the high-field series is the transition $(n = 15, J = 16) \rightarrow (n = 17, J = 16)$ as shown in Figs. 3 and 4, and Table I.

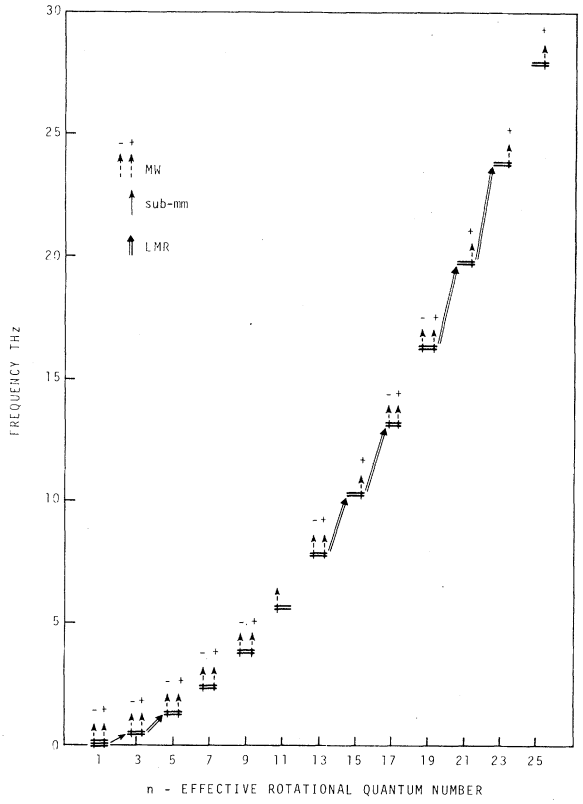

FIG. 1. Rotational energy levels in the electronic and vibration ground state of the oxygen molecule. Vertical arrows indicate observed microwave transition within each triplet (+ and − indicate transitions $J = n + 1$ to $J = n$ and $J = n - 1$ to $J = n$, respectively), an arrow from $n = 1$ to $n = 3$ indicates submillimeter wave transition, and five double arrows indicate transitions observed in LMR spectra.

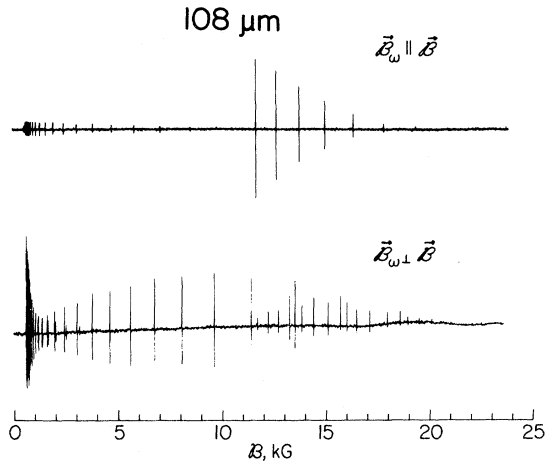

FIG. 2. Chart-recorder traces of the laser magnetic resonance of the O_2 molecule using the 108-μm D_2O laser line. $\mathcal{B}$ is the external magnetic field, while $\mathcal{B}_\omega$ gives the direction of the magnetic component of the laser field.

There exist two conflicting sets of g factors for this molecule:

$$g_\perp = 2.004\,838\,(30)\,, \quad g_z = 2.002\,025\,(20)\,, \quad g_n = 0.000\,126\,(12) \tag{1}$$

proposed by Bauers, Kamper, and Lustig[7] in analyzing their data of microwave electron spin

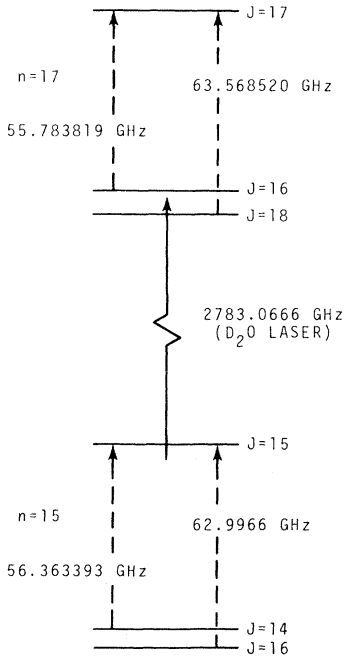

FIG. 3. Triplet levels of $n=15$ and 17. The transition frequencies within each triplet are observed in microwave spectroscopy.

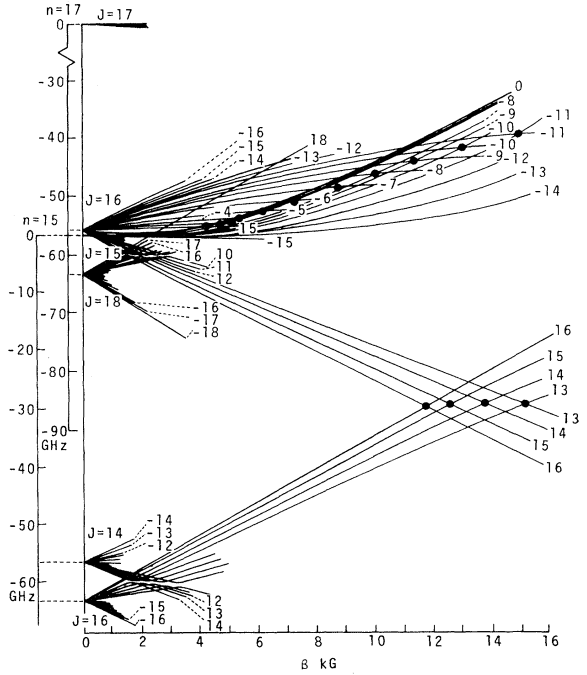

FIG. 4. Schematic energy-level diagram to illustrate the laser magnetic resonances at 108 μm. All the $n=15$ levels are shifted up by the laser frequency so that an appropriate level of $n=15$ crosses the corresponding one of $n=17$ at the resonance field of the transition. Note that the ($n=J=15$) level nearly coincides with the ($n=17$, $J=16$) level in this diagram, and that produces the low-field series of LMR spectrum. Only $M \leq 0$ levels of ($n=J=15$) states are shown explicitly to avoid confusion.

resonance, and subsequently confirmed by Tischer,[8] and

$$g_\perp = 2.005\,169\,(56)\,, \quad g_z = 2.001\,939\,(26)\,, \quad g_n = 0.000\,122\,(15) \tag{2}$$

proposed by Hendrie and Kusch[9] in analyzing their

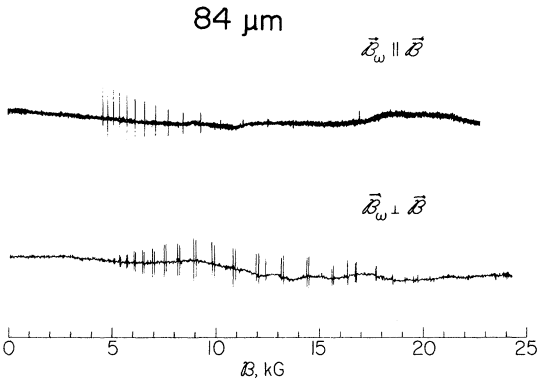

FIG. 5. Chart-recorder traces of the laser magnetic resonance of the O_2 molecule using the 84-μm D_2O laser line.

TABLE I. Resonance fields and their assignments for the oxygen molecule using the 108-μm D_2O laser line. (a) $\vec{\mathcal{B}} \| \vec{\mathcal{B}}_\omega$; (b) $\mathcal{B} \perp \mathcal{B}_\omega$. ($\mathcal{B}$ is the external magnetic field and $\mathcal{B}_\omega$ is the magnetic component of the laser radiation fields.)

(a) $\vec{\mathcal{B}} \| \vec{\mathcal{B}}$

$\mathcal{B}$ (G)	206	221	238	256	279	305	336	375	422	481	559	662	802	998	1272	1652	2158	2798	3578	4501
$M(n=17,J=16)$	15	14	13	12	11	10	9	8	7	6	5	4	3	2	1	0	−1	−2	−3	−4
$M(n=J=15)$	15	14	13	12	11	10	9	8	7	6	5	4	3	2	1	0	−1	−2	−3	−4
$M(n=15,J=16)$																				

$\mathcal{B}$ (G)	5582	6844	8328	10 065	11 547	12 121	12 553	13 687	14 952	16 341	17 834
$M(n=17,J=16)$	−5	−6	−7	−8	16	−9	15	14	13	12	11
$M(n=J=15)$	−5	−6	−7	−8		−9					
$M(n=15,J=16)$					16		15	14	13	12	11

(b) $\mathcal{B} \perp \mathcal{B}$

$\mathcal{B}$ (G)	195	208	222	238	258	280	306	338	376	424	479	485	555	562	655	668	793	810	984	1010	1253
$M(n=17,J=16)$	16	15	14	13	12	11	10	9	8	7	6	6	5	5	4	4	3	3	2	2	1
$M(n=J=15)$	15	14	13	12	11	10	9	8	7	6	7	5	6	4	5	3	4	2	3	1	2
$M(n=15,J=16)$																					

$\mathcal{B}$ (G)	1291	1625	1684	2118	2206	2739	2875	3489	3691	4372	4666	5394	6578	7953	9558	11 442	11 765	12 297	12 816	13 657	13 998
$M(n=17,J=16)$	1	0	0	−1	−1	−2	−2	−3	−3	−4	−4	−5	−6	−7	−8	−9	15	16	14	−10	13
$M(n=J=15)$	0	1	−1	0	−2	−1	−3	−2	−4	−3	−5	−4	−5	−6	−7	−8				−9	
$M(n=15,J=16)$																	16	15	15		14

$\mathcal{B}$ (G)	14 597	15 314	15 937	16 259	16 749	17 385	18 282
$M(n=17,J=16)$	14	12	13	−11	11	12	10
$M(n=J=15)$				−10			
$M(n=15,J=16)$	13	13	12		12	11	11

TABLE II. Zero-field energy separation obtained from LMR (in GHz).

	LMR series	Using Set (1)	Using Set (2)
$\nu((n=J=15)\rightarrow(n=J=17))$	low-field series	2839.4006(6)	2839.4006(6)
	high-field series	2839.404(6)	2839.414(6)
$\nu((n=J=19)\rightarrow(n=J=21))$		3524.221(5)	3524.217(5)

data of molecular-beam magnetic resonance.

Although individual LMR series with an experimental accuracy of ± 0.3 G in the magnetic field and ± 1 MHz in the laser frequency cannot distinguish between sets (1) and (2), in the present case of the 108-μm D_2O laser line we are in a fortunate situation of having two LMR series simultaneously, one of which falls very close to zero field: this leads us to choose set (1) rather than set (2), as is shown below.

Since we need a very short-range extrapolation to obtain zero-field energy separation from the low-field series of LMR measurements, we obtain the zero-field energy separation between $(n=J=15)$ and $(n=17, J=16)$ levels independently of the choice of the values of the g factors, as

$$\nu((n=J=15)\rightarrow(n=17, J=16)) = 2783.6166(6)\ \text{GHz}$$

where the uncertainty is due to the experimental uncertainty. Combining this result with the microwave data for the energy separation between $(n=J=17)$ and $(n=17, J=16)$ levels, we obtain the value of the energy separation between $(n=J=15)$ and $(n=J=17)$ levels as is shown in the first line of Table II. Using the high-field LMR series, we can follow the same procedure to obtain the energy separation between the same pair of levels, and the results are shown in the second line of Table II. By comparing the values in the second line with those in the first line of Table II, we see that set (1) gives a consistent result, and is therefore acceptable, while set (2) does not give a consistent result.

The LMR recorder traces for the 84-μm D_2O laser line (3557.1474 GHz) are shown in Fig. 5. Most of the corresponding transitions are assigned as $(n=19, J=20)\rightarrow(n=21, J=20)$ with appropriate

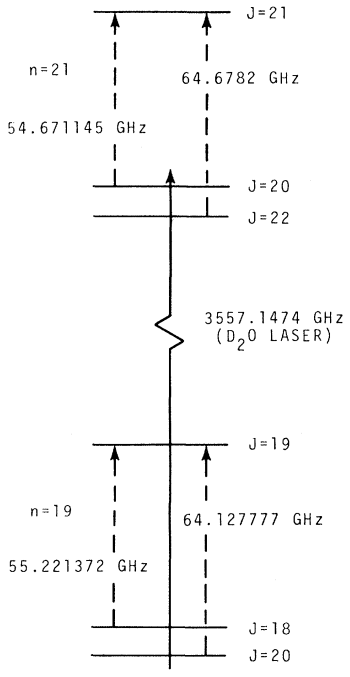

FIG. 6. Triplet levels of $n=19$ and 21.

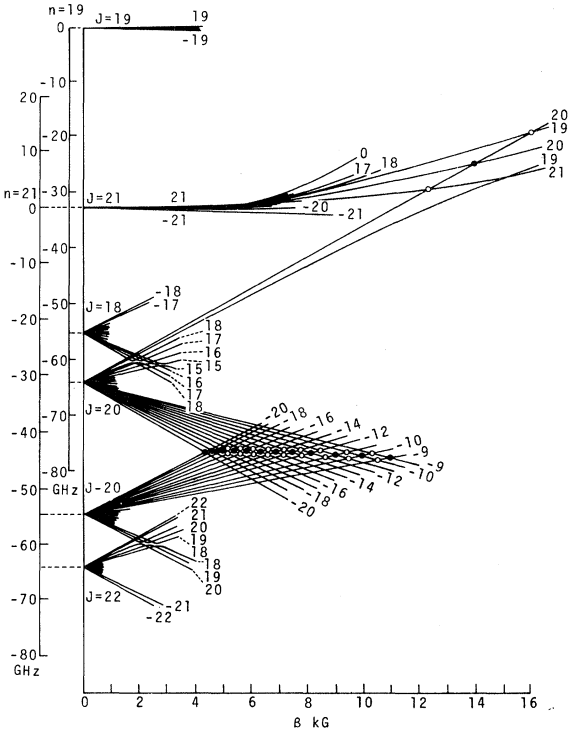

FIG. 7. Schematic energy-level diagram to illustrate the laser magnetic resonances at 84 μm. All the $n=19$ levels are shifted up by the laser frequency. Transitions for $\mathcal{B}\parallel\mathcal{B}_\omega$ and $\mathcal{B}\perp\mathcal{B}_\omega$ cases are indicated by ● and ○, respectively. The transition $(n=19,\ J=M=20)\rightarrow(n=J=21,\ M=20)$ is too weak to be observed.

TABLE III. Resonance fields and their assignments for the oxygen molecule using the 84-μm D_2O line. (a) $\vec{\mathcal{B}} \| \vec{\mathcal{B}}_\omega$; (b) $\vec{\mathcal{B}} \perp \vec{\mathcal{B}}_\omega$.

						(a) $\vec{\mathcal{B}} \| \vec{\mathcal{B}}_\omega$							
$\mathcal{B}$ (G)	4316	4559	4832	5140	5489	5888	6348	6882	7504	8234	9086	10 071	11 188
$M(n=21, J=20)$	−20	−19	−18	−17	−16	−15	−14	−13	−12	−11	−10	−9	−8
$M(n=19, J=20)$	−20	−19	−18	−17	−16	−15	−14	−13	−12	−11	−10	−9	−8
$\mathcal{B}$ (G)	12 410	13 690	14 962	16 163	17 238								
$M(n=21, J=20)$	−7	−6	−5	−4	−3								
$M(n=19, J=20)$	−7	−6	−5	−4	−3								
						(b) $\vec{\mathcal{B}} \perp \vec{\mathcal{B}}_\omega$							
$\mathcal{B}$ (G)	4413	4456	4668	4715	4955	5007	5279	5338	5649	5714	6073	6146	6563
$M(n=J=21)$													
$M(n=21, J=20)$	−20	−19	−19	−18	−18	−17	−17	−16	−16	−15	−15	−14	−14
$M(n=19, J=20)$	−19	−20	−18	−19	−17	−18	−16	−17	−15	−16	−14	−15	−13
$\mathcal{B}$ (G)	6646	7134	7227	7803	7907	8586	8700	9499	9622	10 548	10 676	11 723	11 847
$M(n=J=21)$													
$M(n=21, J=20)$	−13	−13	−12	−12	−11	−11	−10	−10	−9	−9	−8	−8	−7
$M(n=19, J=20)$	−14	−12	−13	−11	−12	−10	−11	−9	−10	−8	−9	−7	−8
$\mathcal{B}$ (G)	12 198	12 984	13 098	14 275	14 371	15 527	15 601	16 300	16 677	16 729	17 682	17 715	
$M(n=J=21)$	21							19					
$M(n=21, J=20)$		−7	−6	−6	−5	−5	−4		−4	−3	−3	−2	
$M(n=19, J=20)$	20	−6	−7	−5	−6	−4	−5	20	−3	−4	−2	−3	

values of M, the magnetic quantum number, as shown in Table III and illustrated in Figs. 6 and 7. There are two lines for the case $\vec{\mathcal{B}} \perp \vec{\mathcal{B}}_\omega$, which are the transitions $(n=19, J=M=20) \rightarrow (n=J=21, M=21$ and 19) as illustrated in Fig. 7. In our previous paper[3] we reported a resonance line at 12.477 kG for the case $\vec{\mathcal{B}} \perp \vec{\mathcal{B}}_\omega$ of the 119-μm H_2O laser line and could not make an assignment. Wayne[10] showed that the line corresponds to the $(n=13, J=M=14) \rightarrow (n=J=M=15)$ transition, and the present two lines are of similar nature.

All resonance lines in the 84-μm spectra are explained within their experimental uncertainty by means of set (1) and set (2). The calculated zero-field energy separation between the $(n=J=19)$ and $(n=J=21)$ levels, obtained by using the LMR data with sets (1) and (2) for the g factors, are given in the last line of Table II, where the uncertainty is due to that of the field measurement. Because of the above discussion on the 108-μm D_2O laser line, the value obtained by using set (1) is believed to be more accurate.

TABLE IV. Experimental and theoretical values of energy separations between $(n=J)$ and $(n'=J')$ rotational levels (in GHz).

n	n'	ν_{expt}	Method	ν_{theor} (Ref. 12)	ν_{theor} (Present)
1	3	430.984 697(60)	Sub-mm	430.9853	430.984 672
3	5	775.6975(70)	LMR	775.7004	775.6992
5	7	1120.30(9)	Raman	1120.2903	1120.288
7	9	1464.63(9)	Raman	1464.6993	1464.696
9	11	1808.84(9)	Raman	1808.8715	1808.867
11	13	2152.77(9)	Raman	2152.7514	2152.745
13	15	2496.283(30)	LMR	2496.2830	2496.275
15	17	2839.4006(6)	LMR	2839.4106	2839.4006
17	19	3182.07(9)	Raman	3182.0782	3182.066
19	21	3524.221(5)	LMR	2524.2300	3524.216
21	23	3865.81(3)	LMR	3865.7970	3865.794

TABLE V. Values of oxygen ($X\ ^3\Sigma_g^-, v=0$) rotational and other parameters (in GHz).

Reference	B_0 (=B)	B_1 (=$-D$) (10^{-4})	B_2 (=H) (10^{-10})	λ_0	λ_1	μ_0	μ_1
Albritton *et al.* (Ref. 13)	43.101 40(80)	−1.451(15)	−0.0114				
Welch and Mizushima (Ref. 12)	43.100 518(3) [a]	−1.449 629(9) [a]	−1.57(11) [a]	59.501 342(7)	$5.847(3)\times10^{-5}$	−0.252 586 5(10)	$-2.464(20)\times10^{-7}$
Evenson and Mizushima (Ref. 3)	43.100518(20) [b]	−1.4496(30) [b]	−1.7(100) [b]				
Present work	43.100 460 8(75) [b]	−1.4520(20) [b]	0 [c]				

[a] Experimental uncertainty is not taken into account in estimating the uncertainties.
[b] Uncertainties are carried over from experimental uncertainty.
[c] $|B_2| < 2\times10^{-10}$ GHz.

All observed energy separations between $(n=J)$ and $(n+2=J+2)$ rotational levels are listed in Table IV. In addition to the LMR and submillimeter data, the less accurate Raman-effect data[11] are also listed in Table IV. According to theory[12] the rotational energy of $(n=J)$ level is given by

$$\epsilon(n=J) = (B_0 + \tfrac{2}{3}\lambda_1 - \mu_1)n(n+1) + B_1[n(n+1)]^2 + B_2[n(n+1)]^3, \quad (3)$$

where B_1 and B_2 are identical to the more conventional notations $-D$ and H, respectively. Since the values of λ_1 and μ_1 are already known from microwave data with sufficient accuracy,[12] we can now find the most plausible values of B_0, B_1, and B_2 by fitting the theoretical formula (3) to the experimental data listed in Table IV. The result is shown in Table V, and the fitting is shown in the last column of Table IV. The present result supersedes the previous results of Welch and Mizushima,[12] and Mizushima and Evenson,[3] since the value of $(n=J=1) \rightarrow (n=J=3)$ has been altered[5] and more data have become available. For comparison we also show the values given by Albritton, Harrop, Schmeltekopf, and Zare[13] in Table V; their values of B_0 and B_1 are obtained by reanalyzing the old spectroscopic data by Babcock and Herzberg,[14] and their value of B_2 is obtained from their RKR potential.

[1] K. M. Evenson, H. P. Broida, J. S. Wells, R. J. Mahler, and M. Mizushima, Phys. Rev. Lett. 21, 1038 (1968).
[2] M. Mizushima, J. S. Wells, K. M. Evenson, and W. M. Welch, Phys. Rev. Lett. 29, 831 (1972).
[3] K. M. Evenson and M. Mizushima, Phys. Rev. A 6, 2197 (1972).
[4] J. S. McKnight and W. Gordy, Phys. Rev. Lett. 21, 1753 (1973).
[5] W. Steinbach and W. Gordy, Phys. Rev. A 8, 1753 (1973).
[6] Particularly, R. W. Zimmerer and M. Mizushima, Phys. Rev. 121, 152 (1961); and B. G. West and M. Mizushima, Phys. Rev. 143, 31 (1966).
[7] K. D. Bauers, R. A. Kamper, and C. D. Lustig, Proc. R. Soc. Lond. A 251, 565 (1959).
[8] R. Tischer, Z. Naturforsch. A 22, 1711 (1967).
[9] J. M. Hendrie and P. Kusch, Phys. Rev. 107, 716 (1957).
[10] D. Wayne (private communication).
[11] R. J. Butcher, D. V. Willetts, and W. J. Jones, Proc. R. Soc. Lond. A 324, 231 (1971).
[12] W. M. Welch and M. Mizushima, Phys. Rev. 143, 31 (1966).
[13] D. L. Albritton, W. J. Harrop, A. L. Schmeltekopf, and R. N. Zare, J. Mol. Spectrosc. 46, 25, 103 (1973).
[14] H. D. Babcock and L. Herzberg, J. Appl. Phys. 108, 167 (1948).